Development status of CLAM steel for fusion application

Qunying Huang *, FDS Team

Institute of Nuclear Energy Safety Technology, Chinese Academy of Sciences, Hefei, Anhui 230031, China

ARTICLE INFO

ABSTRACT

The China low activation martensitic (CLAM) steel is being developed at the Institute of Nuclear Energy Safety Technology (INEST) under wide collaboration within China. Significant R&D work on CLAM steel was carried out to help make it suitable for industrial applications. The effect of refining processes and thermal aging on composition, microstructures and mechanical properties were investigated. Material properties before irradiation including impact, fracture toughness, thermal aging, creep and fatigue properties etc. were assessed. A series of irradiation tests in the fission reactor HFETR in Chengdu up to 2 dpa and in the spallation neutron source SINQ in Paul Scherrer Institute up to 20 dpa were performed. PbLi corrosion tests for more than 10,000 h were done in the DRAGON-I and PICOLO loops. Fabrication techniques for a test blanket module (TBM) are being developed and a 1/3 scale TBM prototype is being fabricated with CLAM steel. Recent progresses on the development status of this steel are presented here. The code qualification of CLAM steel is under plan for its final application in ITER-TBM and DEMO in the future.

© 2014 Elsevier B.V. All rights reserved.

1. Introduction

Reduced activation ferritic/martensitic steels (RAFMs) are considered as one of the most promising structural materials for the future fusion reactors because of their good irradiation swelling resistance, thermo-physical, and thermo-mechanical properties. Great efforts on developing the China low activation martensitic (CLAM) steel have also been made during the past decade at the Institute of Nuclear Energy Safety Technology (INEST), Chinese Academy of Sciences (CAS) under close collaboration with many institutes and universities [1–3]. It has been chosen as the primary candidate structural material in the designs of FDS series PbLi blankets for fusion reactors, dual functional lithium lead (DFLL) test blanket module (TBM) [4–6] for ITER and China fusion engineering test reactor (CFETR) blanket in China [7].

Since the TBMs will be tested in ITER, the properties of CLAM steel have to be evaluated and assessed with French regulations on pressure vessel equipment, possibly in its nuclear extension, as well as high standards of quality assurance required for reliable and safe operation of ITER [8]. A lot of efforts are being devoted on the development of CLAM steel in material fabrication processes, material property evaluation (including corrosion, irradiation, fabrication and compatibility etc.) and the establishment of a material database for its application in ITER CN TBM.

The R&D activities, development status and properties of CLAM steel are reviewed in this paper.

2. CLAM steel

The nominal chemical composition (wt%) of CLAM steel is: 0.1 ± 0.02 C, 9 ± 0.5 Cr, 1.5 ± 0.2 W, 0.15 ± 0.02 Ta, 0.2 ± 0.02 V, 0.45 ± 0.05 Mn, balance Fe. The heat treatment is normalizing at 980 °C for 30 min and then cooling in air to room temperature (RT) and tempering at 760 °C for 90 min and then cooling in air to RT.

Two industrial scale ingots of 1.2 tons and 4.5 tons, named HEAT 0912 and HEAT 1105, respectively, were fabricated with vacuum induction melting (VIM) and vacuum arc remelting (VAR). The chemical compositions of the products were listed in Table 1. The microstructure of as-received CLAM steel was tempered martensite, and the average grain size was ∼10 μm. According to the international standard ISO 4967, the non-metalic inclusion rate was less than 1 for type A, B, C, and D inclusions.

3. Properties tests before irradiation

3.1. Effect of refining processes on tensile and Charpy impact properties

The influence of smelting processes on mechanical properties of CLAM steel was investigated [9]. Four refining processes were

* Address: P.O. Box 1135, No. 350, Shushanhu Road, Hefei, Anhui 230031, China. Tel./fax: +86 551 65593328.
E-mail address: qunying.huang@fds.org.cn

Table 1
Chemical compositions of HEAT 0912 and HEAT 1105 (wt%).

	Cr	W	Ta	V	C	Si	Mn	P	S	O	N	Fe
HEAT 0912	8.86	1.48	0.12	0.21	0.094	0.05	0.48	0.005	0.002	0.004	0.009	Bal.
HEAT 1105	8.76	1.40	0.16	0.22	0.100	0.05	0.42	0.010	0.005	0.006	0.040	Bal.

Table 2
Four refining processes and impurity contents of CLAM steels.

Ingot No.	Refining process	Sum of impurity contents of O, N, S, P (ppm)
CLAM-1	VIM	205
CLAM-2	VIM + ESR	228
CLAM-3	VIM + ESR + VAR	133
CLAM-4	VIM + VAR	205

performed as listed in Table 2. The combination process of VIM, electro-slag remelting (ESR) and VAR could further decrease the total amount of impurity elements including O, N, S and P etc. and obtain more uniform distribution of Ta in the matrix, which led to higher strength and lower ductile brittle transition temperature (DBTT) as shown in Figs. 1 and 2.

3.2. Fatigue properties

The low cycle fatigue (LCF) properties of the CLAM steel were characterized and compared with the results of Eurofer97 [10,11]. These experiments were performed at room temperature (RT) in air under fully reversed push–pull triangular wave. The amplitude of applied strains varies from 0.2% to 2.0%. In the process of LCF at RT, CLAM steels showed cyclic hardening at the beginning (i.e. 1–100 cycles) and then continuous cyclic softening, which was similar to those of Eurofer97 [11]. The effect of axial strains on the numbers of cycles to failure of CLAM and Eurofer97 at different total axial strain ranges were shown in Fig. 3. The data was evaluated with the Coffin–Manson type regression formula:

$$\frac{\Delta\varepsilon_t}{2} = \frac{\Delta\varepsilon_p}{2} + \frac{\Delta\varepsilon_e}{2} = 59.2(2N_f)^{-0.65} + 0.54(2N_f)^{-0.093}$$

where $\frac{\Delta\varepsilon_t}{2}, \frac{\Delta\varepsilon_p}{2}$ and $\frac{\Delta\varepsilon_e}{2}$ are the total, plastic and elastic strain aptitudes, respectively; $2N_f$ is the number of reversals to failure. The transition life (when $\frac{\Delta\varepsilon_p}{2} = \frac{\Delta\varepsilon_e}{2}$) of CLAM steel was ~8000 cycles at RT.

The microstructure evolution in CLAM specimens during the LCF tests was inspected, the decrease in dislocation density and
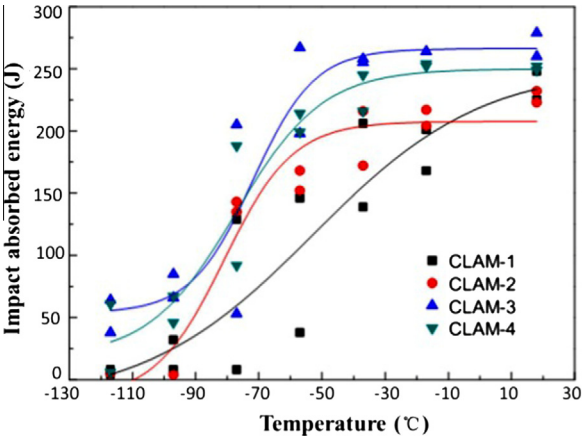

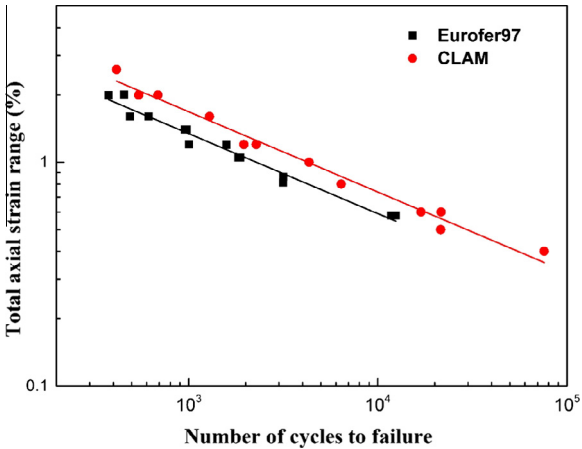**Fig. 2.** Effect of different refining processes on Charpy impact absorbed energy.

Fig. 3. S–N curves of CLAM and Eurofer97 specimens at RT.
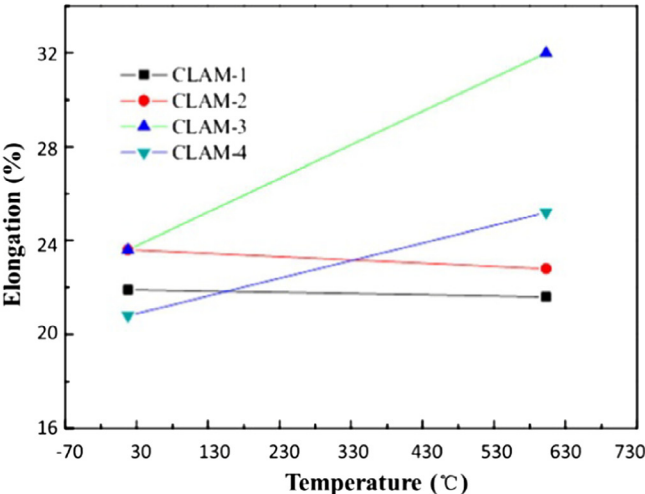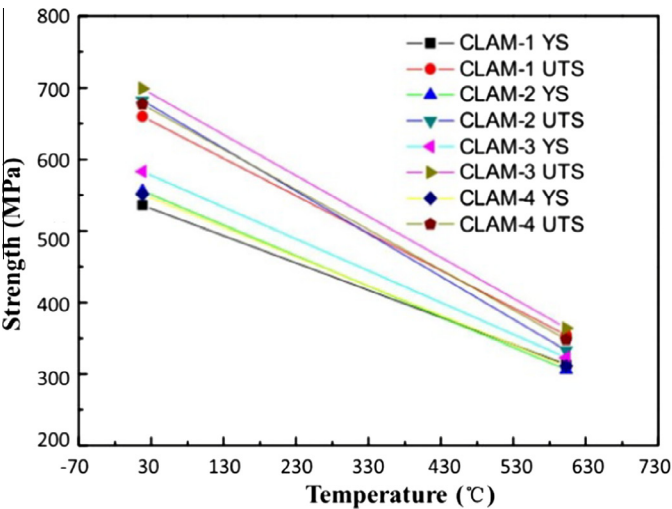

Fig. 1. Effect of different refining processes on tensile properties.

the disappearance of large grains were observed, which were similar to those of Eurofer97 [11].

3.3. Fracture toughness

The fracture toughness is one of the important material parameters to evaluate the performance of structural materials under complex mechanical loads. The fracture tests for CLAM steel were carried out at RT with three compact tension specimens according to ASTM E1820-2011. From the J–R curve shown in Fig. 4, the fracture toughness J_{IC} was 417.9 ± 6.8 kJ/m^2. The microstructure observation on crack surfaces showed that the fracture occurred in a typical ductile fracture mode.

The fracture toughness was calculated on the basis of the fractal dimension by the analysis of fracture surface under plane strain with the vertical section method and image analysis technique [12]. The calculated J_{IC} was 454.59 kJ/m^2 as shown in Fig. 5. The relative error of J_{IC} for the experimental and calculated results was 8.1%.

3.4. Creep property

The creep resistance is one of the most important properties for the application of the RAFMs in fusion reactors under long-time loading at high temperature. The constant load creep tests of CLAM (HEAT 0912) were carried out at 500 °C, 550 °C and 600 °C,
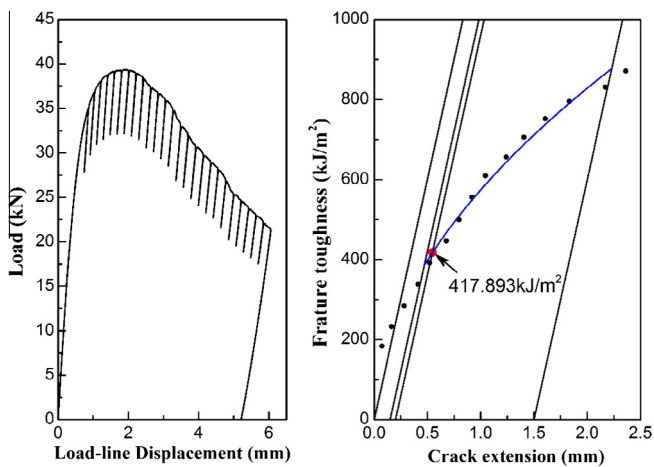
respectively, with stresses ranging from 150 MPa to 300 MPa [13]. The samples for creep testing were round with diameter 5 ± 0.02 mm and the gauge length was 50 ± 0.1 mm. As shown in Fig. 6, the creep curve exhibited three regimes i.e. primary, secondary and tertiary creep, which indicated a normal creep behavior. With the increase in test temperature from 550 °C to 600 °C, the stress exponent n varied from 19 to 15, which was similar to those of the other 9–12 wt% Cr steels [14–17]. The activation energy Q was ~676 kJ/mol at the temperature of 550–600 °C with the constant stress of 200 MPa. The fracture surfaces of specimens were examined by scanning electron microscopy (SEM). The fractographs indicated transgranular fracture under all the test conditions with the character of dimples owing to combination of micro-voids. Similar results in the other 9 wt% Cr martensitic steels were presented in Ref. [18]. Fig. 7 shows the microstructure of a CLAM specimen observed with transmission electron microscopy (TEM) after creep testing at 550 °C with a stress of 200 MPa for 1595 h. The diameter of $M_{23}C_6$ precipitates in the matrix increased from 100–150 nm to ~200 nm during the long-time creep test.

The long-time creep test for CLAM steel e.g. at 550 °C with stress of 150 MPa is underway.

3.5. Thermal aging

Aging effect is another one of the key factors related to the design limit of RAFM steel, because thermal aging could cause significant change of microstructure and then the degradation of the mechanical properties. Investigation on the microstructure
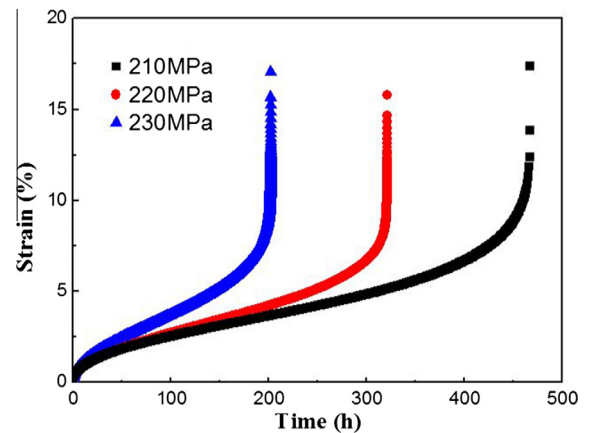

Fig. 4. Load and load-line displacement curve (left) and J–R curve (right).

Fig. 6. Creep curves of CLAM steel at 550 °C.

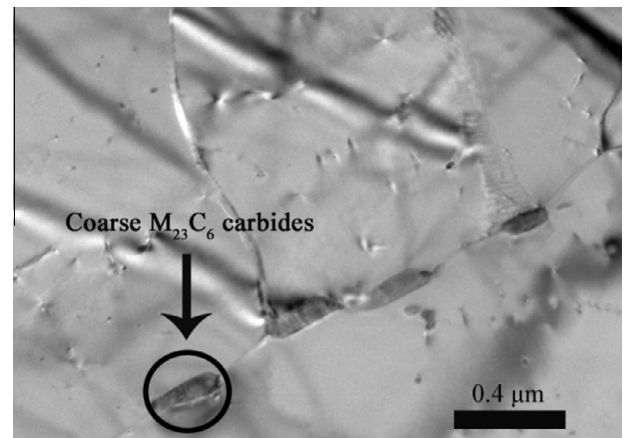**Fig. 5.** Surface roughness vs measurement scale.

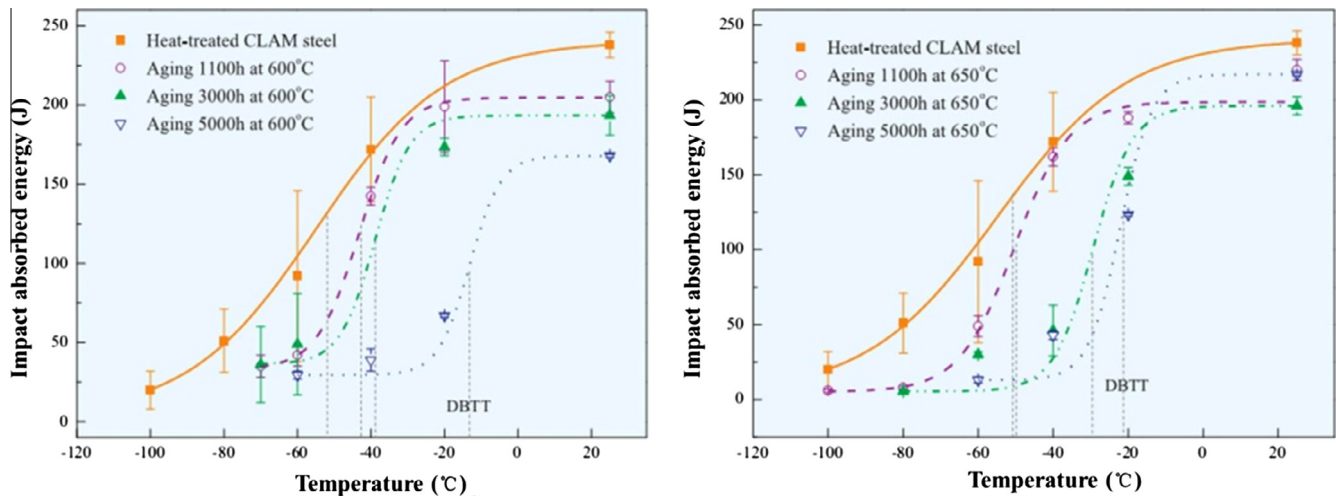**Fig. 7.** Coarse $M_{23}C_6$ carbides on subgrain boundaries.

Fig. 8. Impact energy of CLAM after long-term thermal aging at 600 °C (left) and 650 °C (right).

evolution and their impact on mechanical properties of CLAM steels was carried out in air at 600 °C and 650 °C for 1100 h, 3000 h and 5000 h, respectively, as shown in Fig. 8 [19]. The DBTT of the thermally-aged CLAM specimens increased to about −10 °C and −20 °C after 5000 h aging at 600 °C and 650 °C, respectively. During long-term thermal aging at 600 °C and 650 °C, the $M_{23}C_6$ carbides (60–200 nm) had a strong pinning effect on the migration of the subgrain boundaries while the fine MX carbonitrides (10–40 nm) had negligible effect on grain growth. The Laves-phase showed much slower growth kinetics at 650 °C than that at 600 °C. This indicated that the nose temperature of Laves-phase formation in the CLAM steel was probably lower than 650 °C. The results showed that Laves-phase had a small impact on the strength at the early stage of precipitation, but the formation of Laves-phase was detrimental to the impact toughness.

4. Neutron irradiation tests

High flux experimental test reactor (HFETR) in Chengdu, China and spallation neutron source SINQ in Paul Scherrer Institute (PSI), Switzerland were selected for the irradiation experiments. Doses to 1–2 dpa at 300–500 °C in HFETR and to 3–20 dpa at 100–500 °C in SINQ were performed to study the effect of neutron irradiation on mechanical properties of CLAM steel. A comparison of the tensile strength and Charpy impact results for CLAM (HEAT 0912) before and after the irradiation to 1.25 dpa at 470 °C in HFETR are shown in Fig. 9. Both the ultimate tensile strength

(UTS) and yield stress (YS) after irradiation increased ∼30 MPa when tested at 200 °C/300 °C, and increased ∼150 MPa when tested at RT. The DBTT, obtained at the half of the upper-shelf value, increased ∼10 °C. The temperature $T_{0.89}$ obtained with the lateral expansion curves increased ∼12 °C, the shift of transition curves due to irradiation was small.

Ref. [20] showed that the YS and UTS of Eurofer97 to 2.39 dpa at 300 °C increased ∼350 MPa and ∼250 MPa, respectively, while tested at RT. The DBTT shift of F82H-IEA to 5 dpa at 500 °C was 32 °C [21]. The DBTT shift of OPTIFER increased 25–46 °C with irradiation doses of 0.8–2.4 dpa at 450 °C [22,23]. These results showed that the neutron irradiation resistance of CLAM steel was comparable with those of Eurofer97, F82H-IEA and OPTIFER.

More post irradiation tests for CLAM specimens with higher doses are underway.

5. Compatibility with PbLi

To evaluate the corrosion behavior of CLAM steel exposed to liquid PbLi under the working conditions for ITER DFLL-TBM, a series of tests were performed at 480 °C and 550 °C, respectively, in DRAGON facilities [24–27].

The corrosion experiments were carried out for 10,000 h in flowing PbLi with a velocity of 0.08 m/s at 480 °C for the specimens with dimension of $\varnothing$10 mm × 30 mm in DRAGON-I loop [27]. The dependence of radius changes versus exposure time is shown in Fig. 10. Based on the radius reduction of the specimens, the
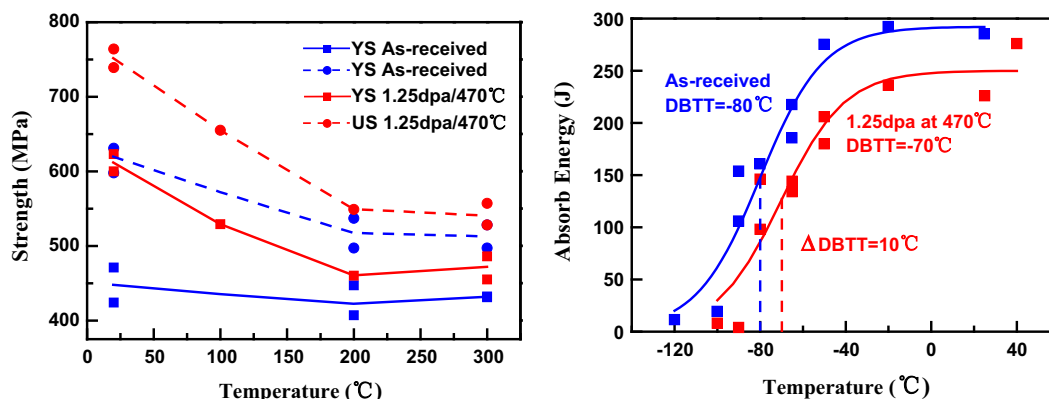

Fig. 9. Tensile strength (left) and Charpy impact energy (right) before and after irradiation.
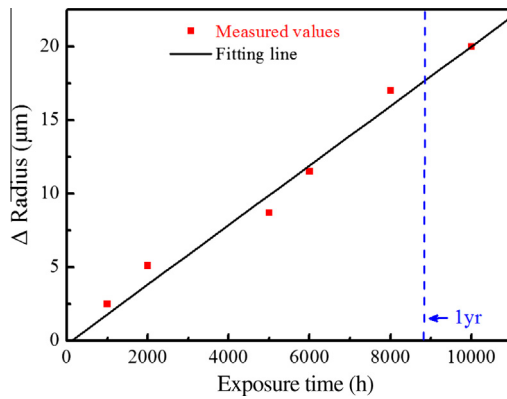
Fig. 10. Radius reduction of the specimens vs. exposure time.

corrosion rate of CLAM steel was calculated to be ~18.5 μm/yr. The composition of the depleted layer on the surface of CLAM steel was analyzed by using SEM with an energy dispersive X-ray (EDX) detector as shown in Fig. 11. The thickness of the depleted layer was 20–30 μm. The porosity in the depleted layer increased with increasing of exposure time.

In order to compare the corrosion behavior of CLAM steel with other RAFM steels, a long-term corrosion test was performed with Eurofer97 specimens at the upper operation temperature of 550 °C for up to 12,000 h in the PICOLO loop at Karlsruhe Institute of Technology (KIT) in Germany with a PbLi flow velocity of 0.10 m/s, which is similar to the conditions in the DFLL-TBM. The results demonstrated that CLAM and Eurofer97 specimens exhibited similar corrosion behavior over the whole test process. The average corrosion rate was ~220 μm/yr for both of the steels [28].

6. Development of TBM fabrication techniques

The fabrication of DFLL-TBM components and related assembly techniques are key issues of TBM technology development. The first wall (FW), the cover plate and cooling plate are the main components of the TBM and contain complex flow channels for helium gas coolant.

The FW was fabricated by hot isostatic pressing (HIP)-diffusion welding (DW) with U-shape rectangular tubes and plates, as shown in Fig. 12 (left). The assembly procedure was as follows: (1) The rectangular tubes and plates were fabricated and formed into U-shape; (2) The tubes and plates were sealed with electron beam welding (EBW) after assembly, and a helium leakage test was performed to assess the sealing quality; (3) After degassing and vacuum sealing, the components were HIPed with parameters

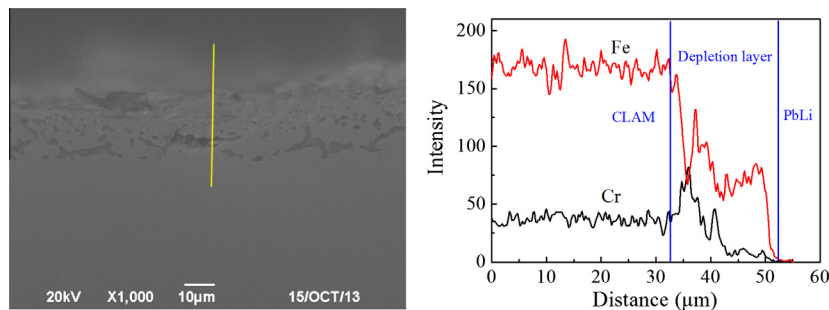**Fig. 13.** 1/3 Scale ITER DFLL-TBM fabricated with CLAM steel.

Fig. 11. SEM micrograph (left) and EDX line scanning analysis (right) on cross-section.
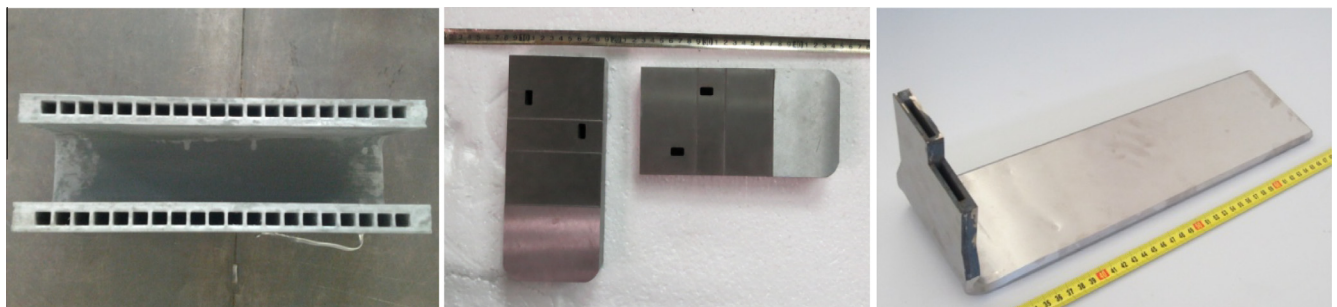

Fig. 12. Photo of the FW (left), cover plates (middle) and the L-shape cooling plate (right).

of 1100 °C/150 MPa/3 h. Non-destructive inspection (i.e. ultrasonic test) showed that the quality of the HIP joints in the FW was sound [29].

For the cover plate and cooling plate, large grooves were made on a thick plate; then, thin strips were used to seal the grooves to form the flow channel; finally, a relatively thick plate was welded on the component with HIP-DW. The photos of the structures were shown in Fig. 12 (middle and right).

EBW and tungsten inert gas (TIG) welding will be the important candidate assembly techniques for ITER-TBM. The assembly of components with cooling channels for 1/3 scale DFLL-TBM was performed (as shown in Fig. 13) with the EB and TIG welding processes. The property tests for the module are underway.

7. Summary

CLAM steel is being developed in INEST under wide collaboration. Great efforts are devoted to its industrial application. Large heats of 1.2 tons and 4.5 tons were fabricated and main compositions were under good control. All round property tests are being performed including a series of neutron irradiation experiments to enrich the database of CLAM. And code qualification of CLAM steel for ITER-TBM is also being pushed forward.

The development of TBM fabrication techniques with CLAM is underway. The 1/3 scale prototypes of the FW, cooling plate and cover panel were performed with one step HIP diffusion welding, and a 1/3 scale DFLL-TBM prototype has been assembled. Full size TBMs will be fabricated in the near future for its final application in ITER and then DEMO.

Acknowledgements

References

[1] Q. Huang, C. Li, Q. Wu, S. Liu, S. Gao, Z. Guo, et al., J. Nucl. Mater. 417 (2011) 85–88.
[2] Q. Huang, N. Baluc, Y. Dai, S. Jitsukawa, A. Kimura, J. Konys, et al., J. Nucl. Mater. 442 (2013) S2–S8.
[3] Q. Huang, C. Li, Y. Li, M. Chen, M. Zhang, L. Peng, et al., J. Nucl. Mater. 367–370 (2007) 142–146.
[4] Y. Wu, FDS Team, J. Nucl. Mater. 367–370 (2007) 1410–1415.
[5] Y. Wu, FDS Team, Nucl. Fusion 47 (2007) 1533–1539.
[6] Q. Huang, Q. Wu, S. Liu, C. Li, B. Huang, L. Peng, et al., Fusion Eng. Des. 86 (2011) 2611–2615.
[7] Y. Wan, Design and strategy for the Chinese Fusion Engineering Testing Reactor (CFETR), presented at the 25th Symposium on Fusion Engineering (SOFE-25), San Francisco, California, USA, June 10–14, 2013.
[8] J.F. Salavy, G. Aiello, P. Aubert, L.V. Boccaccini, M. Daichendt, G. De Dinechin, et al., J. Nucl. Mater. 386–388 (2009) 922–926.
[9] S. Liu, Q. Huang, C. Li, B. Huang, Fusion Eng. Des. 84 (2009) 1214–1218.
[10] X. Hu, L. Huang, W. Wang, Z. Yang, W. Sha, W. Wang, et al., Fusion Eng. Des. 88 (2013) 3050–3059.
[11] P. Marmy, T. Kruml, J. Nucl. Mater. 377 (2008) 52–58.
[12] B. Pramanik, T. Tadepalli, P.R. Mantena, Materials 5 (2012) 922–936.
[13] B. Zhong, B. Huang, S. Liu, C. Li, G. Xu, Q. Huang, Creep deformation and rupture behavior of CLAM steel at 823 K and 873 K, J. Nucl. Mater. 455 (1–3) (2014) 640–644.
[14] B.K. Choudhary, E. Isaac Samuel, J. Nucl. Mater. 412 (2011) 82–89.
[15] K. Kimura, K. Sawada, H. Kushima, T. Indian I. Metals 63 (2010) 123–129.
[16] K. Sawada, K. Kubo, F. Abe, Mater. Sci. Eng.: A 319 (2001) 784–787.
[17] F. Abe, Mater. Sci. Eng.: A 319 (2001) 770–773.
[18] T. Shrestha, M. Basirat, I. Charit, G.P. Potirniche, K.K. Rink, Mater. Sci. Eng.: A 565 (2013) 382–391.
[19] X. Hu, L. Huang, W. Yan, W. Wang, W. Sha, Y. Shan, et al., Mater. Sci. Eng.: A 586 (2013) 253–258.
[20] J. Rensman, E. Lucon, J. Boskeljon, J. van Hoepen, R. den Boef, P. ten Pierick, J. Nucl. Mater. 239–333 (2004) 1113–1116.
[21] M.A. Sokolov, H. Tanigawa, G.R. Odette, K. Shiba, R.L. Klueh, J. Nucl. Mater. 367–370 (2007) 68–73.
[22] H.C. Schneider, B. Dafferner, J. Aktaa, J. Nucl. Mater. 321 (2003) 135–140.
[23] H.C. Schneider, B. Dafferner, J. Aktaa, J. Nucl. Mater. 295 (2001) 16–20.
[24] Q. Huang, S. Gao, Z. Zhu, M. Zhang, Y. Song, C. Li, et al., Fusion Eng. Des. 84 (2009) 242–246.
[25] Q. Huang, M. Zhang, Z. Zhu, S. Gao, Y. Wu, Y. Li, et al., Fusion Eng. Des. 82 (2007) 2655–2659.
[26] M. Zhang, Q. Huang, Y. Wu, Z. Zhu, S. Gao, Y. Song, et al., Mater. Sci. Forum 561–565 (2007) 1741–1744.
[27] Z. Zhu, M. Zhang, S. Gao, Y. Song, C. Li, L. Peng, et al., Fusion Eng. Des. 84 (2009) 5–8.
[28] J. Konys, W. Krauss, Z. Zhu, Q. Huang, Comparison of corrosion behavior of EUROFER and CLAM steels in flowing Pb-15.7Li, J. Nucl. Mater. 455 (1–3) (2014) 491–495.
[29] C. Li, B. Huang, J. Zhang, Y. Zhai, Q. Wu, S. Liu, et al., Fabrication techniques development of dual functional lithium lead test blanket module in China, http://dx.doi.org/10.13182/FST13-769.